International Food Research Journal 28(4): 860 - 870 (August 2021)
Journal homepage: *http://www.ifrj.upm.edu.my*

Optimisation of alginate-pectin bead formulation using central composite design guided electrospray technique

[1]Azhar, M. F., [2]*Haris, M. S., [1]Mohamad, I. [1]Ismadi, M. N. S., [1]Yazid, A. A. H., [1]Rahman, S. R. and [1]Azlan, N. H.

[1]*Laboratory of Advanced Drug Delivery, Kulliyyah of Pharmacy, International Islamic University Malaysia, Jalan Sultan Ahmad Shah, 25200 Kuantan, Pahang, Malaysia*
[2]*Department of Pharmaceutical Technology, Kulliyyah of Pharmacy, International Islamic University Malaysia, Jalan Sultan Ahmad Shah, 25200 Kuantan, Pahang, Malaysia*

Article history

Received: 3 September 2020
Received in revised form: 18 October 2020
Accepted: 7 November 2020

Keywords

alginate, pectin, electrospray, central composite design, sphericity

Abstract

Alginate-pectin beads act as a carrier in improving the oral bioavailability of bioactive compounds. Electrospray technique facilitates the production of uniform size and shape of alginate-pectin beads. Interaction between key electrospray process parameters affects the size and shape of the beads. A proper model should be employed to establish these correlating interactions. In the present work, the electrospray technique was guided with a central composite design (CCD) and response surface methodology (RSM). One quadratic and one linear model were obtained for size and sphericity coefficient, respectively. The CCD-RSM empirical model derived from the present work is essential to determine the significant factors and their levels in producing beads with consistent size and sphericity coefficient. The results indicated that the applied voltage had the most significant influence on size, while the alginate-pectin concentration was the most prominent factor in producing spherical beads. Spherical beads with a minimum size of 2.97 mm were obtained at an alginate-pectin concentration of 3.5%, a flow rate of 10.0 mL/h, an applied voltage of 2.4 kV, and a distance between the nozzle and the gelation bath of 16.0 cm.

Introduction

Alginate is a polysaccharide derived from brown algae, predominantly *Laminaria hyperborea, Azotobacter vinelandii*, and several *Pseudomonas species* as the main component in their protective biofilm (Setyawidati *et al.,* 2018). Alginate has become one of the most widely commercially used polymers in various fields; the pharmaceutical field first applied alginate to encapsulate islet cells in a study, which resulted in the maintenance of its morphology and functions over 15 min. This finding led to the implementation of alginate in the pharmaceutical industry as a beneficial encapsulating matrix for improving the stability of materials (Lim and Sun, 1980).

However, despite the single use of biopolymer as the standard hydrogel carrier, there are ongoing studies on two or more matrices to form mixed gels of interest (Kennedy *et al.,* 2015; Dekkers *et al.,* 2016). These synergistic mixed gels can potentially produce microstructures and textures that are distinctive from those of pure gels, thus further improving the product quality. Further reduction in production cost can be obtained since the synergistic mixed gel can manifest better rheological properties during the manufacturing process (Walkenström *et al.,* 2003). There are numerous reviews on the synergistic interaction between two different chemical groups of matrices such as polygalactans, and galacto- and glucomannans (Chakraborty, 2017).

Uniquely, alginate and pectin create mixed beads that act synergistically under acidic conditions. The pH value critically contributes to the generation of relatively non-breakable gels; ideally, a pH value below 4 favours gel formation (Guo and Kalentunc, 2016). The gel characteristics are profusely dependent on the intrinsic chemistry of the alginate and pectin samples being mixed. Cohesive gel networks can be produced with a high degree of pectin esterification with guluronate residue of alginate (Guo *et al.,* 2018). The gel firmness is also affected by other external parameters such as the concentration of the participating hydrocolloids and their ratio, ions present in the crosslinking bath, and most prominently, the pH of the gelling environment (Aguilar *et al.,* 2015). It has conclusively been shown that an ideal ratio of 1:1 generated alginate-pectin beads with the highest gel

*Corresponding author.
Email: solah@iium.edu.my

DOI: https://doi.org/10.47836/ifrj.28.4.22

strength (Walkenström *et al.,* 2003).

Alginate-pectin bead size and sphericity are the two major parameters for both food and pharmaceutical applications in encapsulating any active ingredient in the mixed gel carrier (Partovinia and Vatankhah, 2019). Generating a smaller bead size is better because a higher resistance towards shear stress and a compressive force can be achieved, thus rendering it to be less immunogenic in the human body. The reduction of bead size can also aid the mass transfer and substrate diffusion phenomena of the active ingredients encapsulated in the alginate-pectin beads (Valente *et al.,* 2019). Regarding the sphericity of the beads, this shape behaviour has an important role in affecting the chemical and mechanical stability. More recent studies have confirmed that stronger and firmer gel networks are generated in nearly spherical beads in comparison to non-spherical beads. Consecutively, the non-spherical ones are more prone to breakage, thus resulting in the release of the encapsulated ingredient while being manufactured (Voo *et al.,* 2016).

The electrospray technique applies the electrohydrodynamic principle, where a precursor solution is forcefully ejected into a ground collector. As the droplet discharged into the ground collector contains solutions, microparticle- or nanoparticle-sized spherical beads appear gradually as electrostatic forces stretch over the surface tension. It is frequently implemented because of its advantageous characteristics of being time-efficient, easy to handle, and non-destructive (Kilinc *et al.,* 2016).

Currently, general research in pharmaceutical and nutraceutical formulation of alginate-pectin bead is still in its infancy. To the best of the authors' knowledge, there is no published analysis on the factors affecting the optimisation of alginate and pectin using electrospraying technique. Therefore, the present work was carried out to determine the critical parameters and their interaction variables involved. Response surface methodology (RSM) by central composite design (CCD) was utilised with the aid of Design Expert® software to develop an accurate and precise model (Sodeifian *et al.,* 2016a; Jafari *et al.,* 2017; Ghelich *et al.,* 2019). The main advantage of RSM is the number of experiments required can be significantly reduced for the optimisation process (Sodeifian *et al.,* 2016b; Coelho *et al.,* 2019). In the present work, there were four variables being manipulated: the concentration of alginate-pectin solution, the applied voltage, the feeding rate of the polymer solution, and the distance between the nozzle and the cross-linking bath, with three fixed parameters which were nozzle size of 22G, concentration of the crosslinking bath of 2.0% calcium chloride, and time of gelation of 30 min throughout 30 runs.

Materials and methods

Materials

Sodium alginate derived from brown algae with a molecular weight of 216.12 g/mol and M/G ratio of 1.60 (certified purity = 85.6%), and pectin derived from citrus peel (degree of esterification = 85%) were purchased from Sigma-Aldrich (Germany). Calcium chloride ($CaCl_2.2H_2O$) anhydrous powder was purchased from Merck (USA).

Preparation of alginate-pectin hydrogel beads

Alginate-pectin solutions with different concentrations of 2, 2.5, 3, 3.5, and 4.0% (w/v) were prepared by mixing equal amounts of sodium alginate and pectin powder at a ratio of 1:1 in distilled water, and continuously stirring for 1 h using a magnetic stirrer (Daihan Labtech; Gyeonggi-do, Republic of Korea), with speed of 5, before electrospraying to ensure homogenous dissolution. Each solution was individually transferred to a 10 mL syringe (Terumo®) that was connected to a silicon tube and 22G nozzle to enhance the flowability of the solution into the gelling bath. An infusion pump was used to aid the alginate-pectin solution to be drawn at a flow rate of interest. A strong electric field was applied between the nozzle and the 6-well beaker containing 2% (w/v) calcium chloride solution as the gelling solution. Calcium-alginate-pectin hydrogel beads instantaneously formed in the solution, and were left to harden for 1 h to obtain optimal gel strength. The beads were washed using distilled water before being collected and stored for further examination. It is noteworthy that the electrospraying process of alginate-pectin beads was done at temperatures of 25 - 30°C.

Determination of alginate-pectin bead diameter

Thirty beads of each formulation were harvested and re-washed with distilled water for image capturing that was conducted at fixed lighting and distance. They were randomly sampled to measure their particle size using image analysis software (Image J; National Institute of Health, USA). Ferret's diameter of each of the bead was measured by the software, and statistical data such as mean, median, and mode were generated automatically.

Determination of surface morphology of alginate-pectin beads

For proper dehydration of the sample,

alginate-pectin beads were rinsed with an increasing gradient of ethanol concentration of 10, 50, 70, 90, and 100%, and left to air dry for 30 min at room temperature (25 - 30°C). Approximately, ten of the alginate-pectin beads were randomly sampled for surface morphology analysis using a scanning electron microscope at 100× and 500× magnification (SEM, Fei, Quanta 450, Thermo Fisher Scientific, Oregon, USA).

Determination of sphericity coefficient (SC) of alginate-pectin beads

The sphericity coefficient of alginate-pectin beads was calculated using the following equation by Houghton and Amidon (1992) (Eq.1):

$$SC = \frac{dmin}{dmax} \quad \text{(Eq. 1)}$$

where, d_{min} and d_{max} = minimum and maximum Ferret's diameters of the alginate-pectin beads, respectively. Beads with a SC value approaching 1 were considered ideal and spherical.

Experimental design

To conduct a simultaneous investigation of influential variables impacting the determination of the ideal size and shape behaviour of alginate-pectin hydrogel beads, CCD was employed. The total number of runs in the CCD was calculated by $2^k + 2k + n0$, where k and n0 were the numbers of critical factors and replications at the centre point. When k = 4 and n0 = 6, 30 runs resulted of the experiment in a single block. Table 1 depicts a CCD of different factors (k) such as alginate-pectin concentration, flow rate of alginate-pectin solution, voltage applied, and distance between the metal capillary and calcium chloride solution, constructed using Design Expert® version 7 software (Stat-Ease, Inc., Minneapolis, USA).

Optimisation of bead diameter and sphericity coefficient

The optimal conditions for the four manipulated variables to create alginate-pectin beads with the smallest bead diameter and the highest sphericity coefficient were generated based on the data input of the initial 30 runs using Design Expert® software.

Validation of the proposed models

To validate the model for bead size, the minimum diameter was preferred (2.877 mm), with another two randomly selected diameters, 2.909 and 2.978 mm. For the sphericity coefficient, a maximum value of 0.763 was chosen.

Results and discussion

Surface morphology analysis of alginate-pectin beads

All alginate-pectin hydrogel solutions with the designated conditions suggested by the Design Expert® software were successfully electrosprayed. The average Ferret's diameter and sphericity coefficient of each alginate-pectin bead were measured using the Image J software. Optical images, size distribution, and SEM photographs of some selected samples are depicted in Figures 1 and 2.

It is crucial to note that the use of increasing concentrations of analytical-grade ethanol to rinse the alginate-pectin bead samples for the dehydration process before SEM imaging caused inconsistent results. The presence of water molecules embedded on the alginate-pectin bead surface was eliminated, which later provoked the shrinkage phenomenon and decreased their size. Consequently, the size of the alginate-pectin beads depicted in the SEM photographs appeared undersized as compared to the original size of the optical images.

Particle size analysis of alginate-pectin beads
Model generation and statistical analysis

The Design Expert® software suggested a second-order polynomial model as the best-fit equation for the particle size of alginate-pectin beads. The accuracy was estimated by applying Fisher's *F*-test to the predicted model. The *F*-value and *p*-value were 3.14 and less than 0.05, respectively,

Table 1. Central composite design for four critical factors in Design Expert® software.

Factor	-α	-1	0	+1	+α
Alginate-pectin concentration (%, w/v)	2.0	2.5	3.0	3.5	4.0
Flow rate of alginate-pectin solution (mL/h)	8	10	12	14	16
Voltage applied (kV)	1.8	2.0	2.2	2.4	2.6
Distance between metal capillary and calcium chloride solution (cm)	12	14	16	18	20

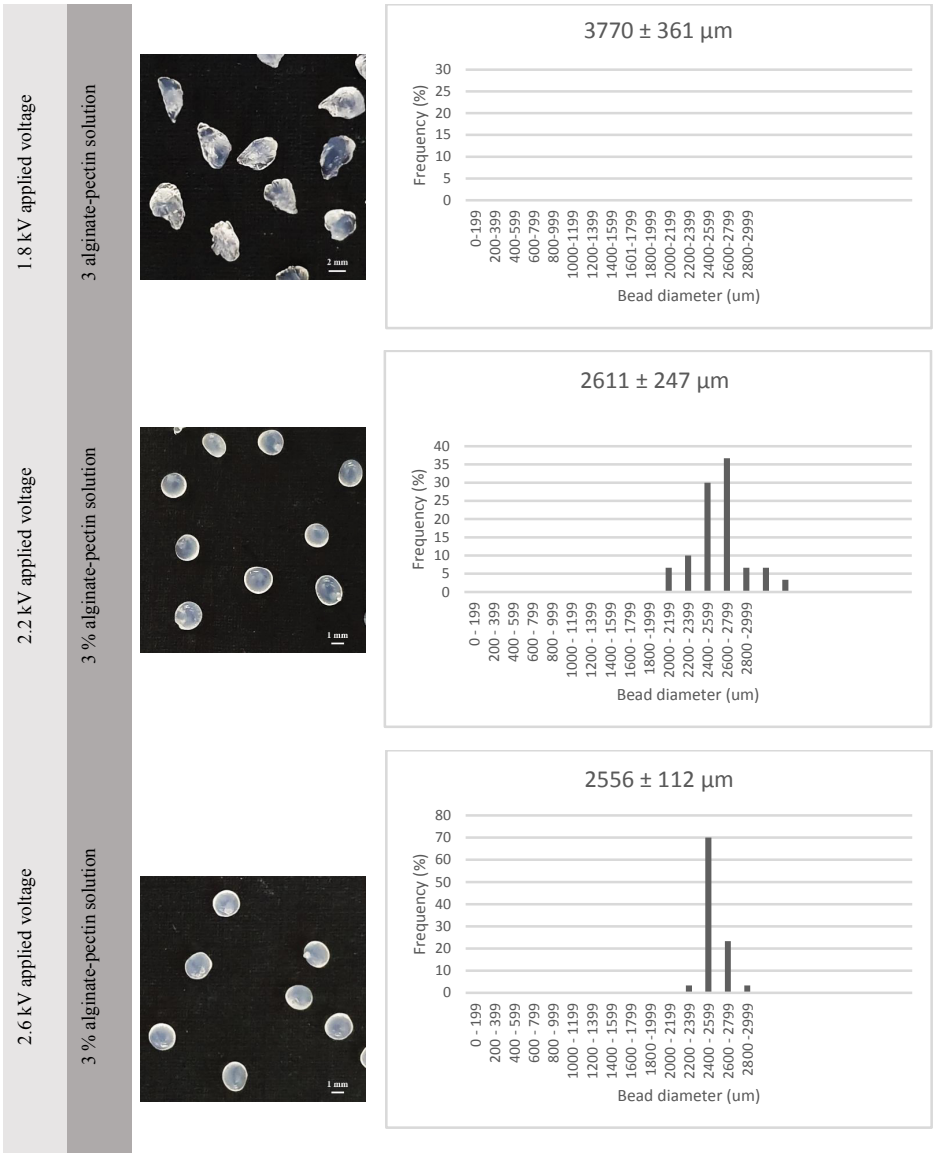

Figure 1. Optical images and size distributions of alginate-pectin beads of selected samples at three different applied voltages (1.8, 2.2, and 2.6 kV).

which indicated the significance of this model.

The significance of manipulated variables and their interacting behaviours in this model were also investigated ($p < 0.05$). Any terms with a *p*-value greater than 0.1 were removed from the model. The "lack of fit *F*-value" of 0.72 indicated that the Lack of Fit was insignificant relative to the pure error, which was good because the model was desirably fit.

Fitness values and consistency were evaluated by multiple coefficients of determination, $R^2 = 0.3955$, alluding to an acceptable correlation between the results predicted by the Design Expert® software with the actual findings. Eq. 2 illustrates the particle size of the alginate-pectin beads in terms of the effective factors (Eq. 2):

$$\text{Particle size (mm)} = 3.44 - 0.091A + 0.048B - 0.16C - 0.12"A^2 - 0.13B^2 \quad \text{(Eq. 2)}$$

Study of manipulated variables and their interacting behaviours

Several researchers have investigated the effects of diverse factors on particle size utilising one-factor-at-a-time (OFAT) experimentation (Vicini *et al.,* 2015; Abyadeh *et al.,* 2017). However, the electrospray technique involves several factors that may affect the process outcomes (Bock *et al.,* 2011). Apart from the main variables, the present work also discussed the effects of interaction between effective variables, particularly the diameter and sphericity of the alginate-pectin hydrogel beads. From Table 1, it was found that the applied voltage (C) had a significant influence ($p < 0.05$) on the particle size. In contrast, no significant effect was

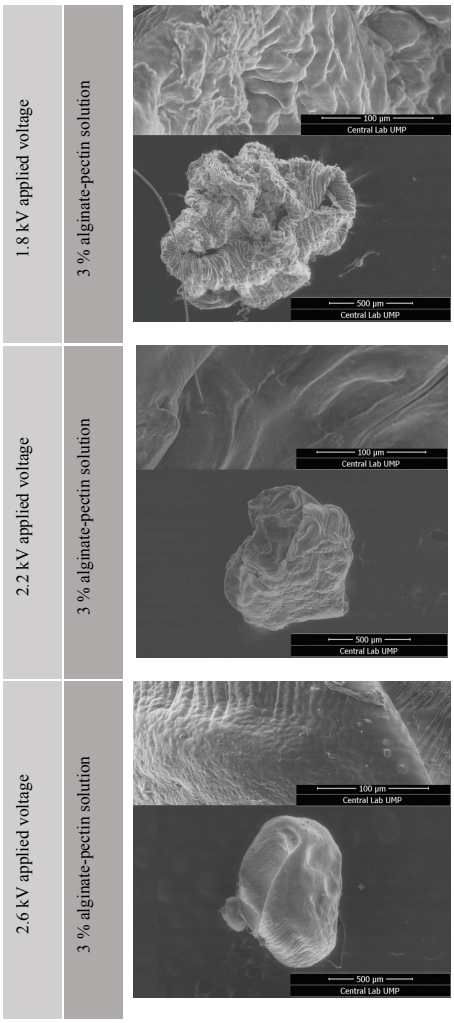

Figure 2. SEM photographs of alginate-pectin beads of selected samples at three different applied voltages (1.8, 2.2, and 2.6 kV).

exerted by other variables, such as the alginate-pectin concentration (A) and flow rate (B). Applied voltage has also been reported by a study to be one of the significant factors that affect the particle size of polymer beads.

A perturbation plot is used to observe the response changes as the level of a factor is manipulated while other related factors are made constant at the optimum level (Oladipo and Gazi, 2015). The response factor sensitivity can be observed by a steep slope in the plot (Anuar *et al.,* 2013). It was revealed that the applied voltage had a dominant effect in terms of particle size as compared to alginate-pectin concentration and flow rate. From the plot, the particle size decreased as applied voltage increased from the optimum value (2.40 kV). This result is similar to a study in which the minimum size of beads was obtained at 2 - 4 kV (Partovinia and Vatankhah, 2019).

Additionally, a reduction in particle size was observed when the concentration of the alginate-pectin solution increased. This result contradicts a study that showed an increasing trend in particle size of alginate hydrogel beads when the polymer concentration was increased from 1.5 to 3% (Mehregan *et al.,* 2016). That study also stated that the more viscous nature of polymer found in higher concentrations of the alginate hydrogel solution might be the main contributor to this phenomenon. Another study also supported that the diameter of beads increased as the alginate concentration increased, which resulted from the increase in viscosity of the gel formed (Lotfipour *et al.,* 2012).

The findings illustrate that when the flow rate of the alginate-pectin solution increased, the particle size of the beads obtained was larger. It has been stated that the coalescence and aggregation phenomenon is more likely to occur with an increase in the flow rate (Yeo and Lim, 2016). Another study reported that the flow rate of the polymer solution did not have a consequential effect on the particle size of the beads formed. That study also revealed that there was only a minimal increase in particle size when the flow rate increased from 3 to 20 mL/h (Ma *et al.,* 2018).

According to the results obtained in the present work, significant interaction behaviours between alginate-pectin concentration and flow rate were observed. In general, it was found that at a flow rate of 10 mL/h, the increase in alginate-pectin concentration increased the particle size of the alginate-pectin beads. From the plot, the largest particle size was obtained at the middle value of alginate-pectin level, which was 2.9 to 3.10%. This finding is in accordance with other studies (Lotfipour *et al.,* 2012; Mehregan *et al.,* 2016; Partovinia and Vatankhah, 2019). However, the particle size then declined as the alginate-pectin concentration was further increased to 3.5%.

The increase in particle size that resulted in the increase in concentration is due to the high viscosity of the polymer present (Ma *et al.,* 2018). A study mentioned that a decrease in particle size could be observed at a lower concentration of alginate-pectin, which is due to the change in polymer concentration, and consequently changes the viscosity more significantly in comparison to the change in conductivity. In the same study, it was explained that the decrease in viscosity resulting from the reduction in concentration produced smaller particle sizes of the beads. However, due to the destabilisation phenomenon, larger beads could also be obtained with a further decrease in viscosity (Abyadeh *et al.,* 2017).

The present work showed variations in particle size at an alginate-pectin concentration of 2.5%; the higher the flow rate of alginate-pectin solution, the larger the particle size of the beads. The maximum particle size of alginate-pectin beads was achieved at a flow rate of approximately 12 mL/h, and consequently decreased when the flow rate further increased to 14 mL/h. This result resembles the findings of a study where it was found that a smaller droplet size was produced when the frequency of hydrogel formation and the flow rate were increased (Bock *et al.,* 2012; Thien *et al.,* 2012). Another study also stated that as the flow rate increased, the frequency of droplet formation would also increase, which resulted in the reduction of the surface charge density of the particle, thus producing beads of large particle sizes (Partovinia and Vatankhah, 2019).

Optimisation of particle size and model validation

For optimisation of the particle size and validation of the model, three validation experiments were conducted. A minimum diameter of 2.877 mm and two randomly selected diameters, which were 2.909 and 2.978 mm, were used. The first validation experiment was carried out under the optimised variable whereas the second and third experiments were chosen randomly. For the first experiment with the highest desirability value of 0.711, electrospraying was carried out under the optimal conditions as suggested by Design Expert® software. The conditions were set at 3.50% alginate-pectin concentration, 10 mL/h flow rate, 2.40 kV of applied voltage, and 16.0 cm distance. The diameter of particles produced was 2.97 mm. Thus, the relative error calculated between the experimental finding and predicted result in these optimised conditions was 3.23%, which indicated a significant correlation between both factors.

Meanwhile, for the second and third validation experiments, with a desirability values of 0.701 and 0.677, respectively, the average diameter

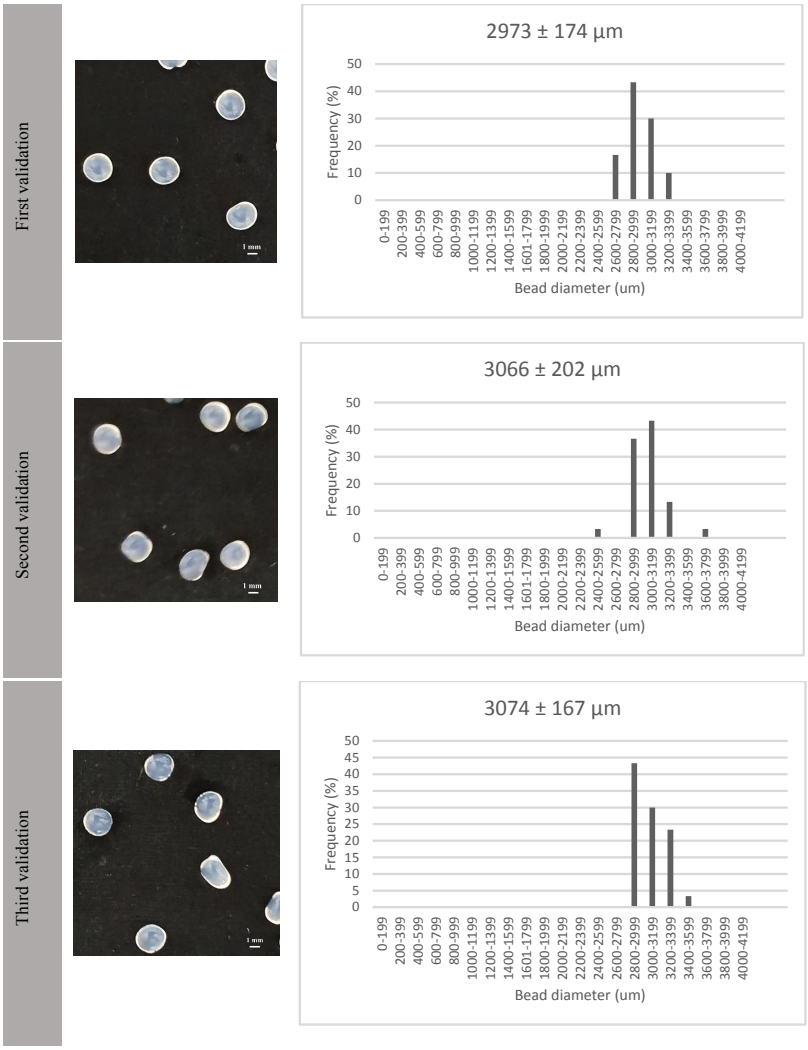

Figure 3. Optical images and size distributions of alginate-pectin beads as validation experiments at desirability values of 0.711, 0.701, and 0.677, respectively.

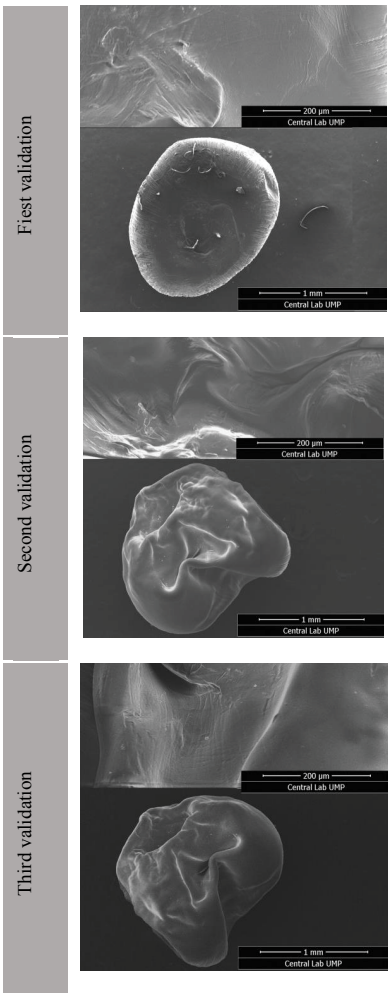

Figure 4. SEM photographs of alginate-pectin beads as validation experiments at desirability values of 0.711, 0.701, and 0.677, respectively.

of particle beads formed was 3.07 and 3.13 mm, respectively. These produced a relative error of 5.53 and 3.09%, respectively, which were still within the accepted range. It can be summarised that all relative error values measured for these validation experiments were within the acceptable range, which confirmed the reliability of the model. Figures 3 and 4 show the optical images, size distribution, and SEM photographs of the alginate-pectin beads from the validation experiments.

Sphericity coefficient analysis of alginate-pectin beads

Model generation and statistical analysis

The software proposed a linear model as the best-fit equation for the sphericity coefficient for alginate-pectin beads. The linear model ws the only significant model with *F*-value of 0.67, *p*-value of 0.7653, and R^2 of 0.2174. According to the ANOVA results, an *F*-value of 6.18 indicated that the model was significant. Additionally, values of "Prob > *F*" less than 0.0500 indicated that the model terms were significant. In this model, alginate-pectin concentration was the only significant model term with "Prob > *F*" value less than 0.05 (0.0192), while other model terms were not significant and had been removed to improve the accuracy. Besides that, the "lack of fit *F*-value" of 0.62 implied that the lack of fit was not significant relative to the pure error since there was 80.52% chance that "lack of fit F-value" this large could occur due to noise.

Furthermore, the "Predicted R^2" of this model was 0.0872, and in consistent agreement with the "Adjusted R^2" of 0.1515. Next, "Adequate Precision" was used to calculate the signal-to-noise ratio, and only a ratio greater than 4 was preferably desirable. In this model, the ratio was 7.859, thus suggesting an adequate signal, and this model could navigate the design space. The sphericity coefficient in terms of actual factors is described in Eq. 3:

Sphericity coefficient = 0.50569850177088 + 0.0 73755239826715A (Eq. 3)

Study of manipulated variables and their interacting behaviours

It was found that the increase in alginate-pectin concentrations yielded a higher sphericity coefficient for the alginate-pectin beads. The steeper the gradient of the perturbation graph, the higher the sensitivity of the graph (Partovinia and Vatankhah, 2019). Meanwhile, the flow rate, applied voltage, and distance between the nozzle and cross-linking solution did not significantly affect the sphericity coefficient. Therefore, alginate-pectin concentration was the main variable that influenced the sphericity coefficient of the alginate-pectin beads.

Similarly, there was only one significant factor that influenced the sphericity coefficient of the alginate-pectin beads, which was alginate-pectin concentration. As the concentration of alginate-pectin solution increased, the sphericity coefficient of the electrosprayed alginate-pectin beads also increased regardless of the flow rate of the alginate-pectin solution. The increase in the flow rate from 10 to 14 mL/h did not affect the sphericity coefficient of beads, as it yielded approximately the same sphericity coefficient value with fixed polymer concentration. For example, when the alginate-pectin concentration was 2.5% (w/v), the sphericity coefficient obtained was approximately 0.69, regardless of the flow rate increment from 10 to 14 mL/h. This finding is consistent with a study which stated that the factors associated with viscosity

affects the spherical shape of beads produced (Partovinia and Vatankhah, 2019).

The highest sphericity coefficient (0.76) was produced when the highest alginate-pectin concentration was used, which was 3.5% (w/v). According to a study, the ability of higher concentration beads to retain their spherical shape is due to the viscous and sticky consistency of the solution (Shi *et al.,* 2011). Upon entering the cross-linking bath, which was the calcium chloride solution, the alginate-pectin beads were exposed to the external drag force by the surrounding calcium chloride solution. However, the internal viscous force maintained a spherical shape within the beads (Lee *et al.,* 2013). The less viscous solution (lower concentration solution) was unable to retain the spherical shape when the solution touched the crosslinking solution, the calcium chloride solution. This could be due to the fact the spherical shape of the alginate-pectin beads was easily disrupted by the drag force exerted by calcium chloride solution (Lee *et al.,* 2013).

A similar study also explained that the concentration of alginate solution is essential because during deformation, the calcium chloride may change the conformation of the alginate molecule if the alginate concentration is too low (Lim *et al.,* 2016). Therefore, a higher concentration of alginate solution can retain the spherical shape because a higher viscosity of alginate can provide adequate strength to the membrane around the beads. The membrane of the alginate bead membrane with greater strength can better protect against the penetration of calcium chloride solution, which can disturb the sphericity of the alginate beads (Abang *et al.,* 2012; Lim *et al.,* 2016).

However, the result obtained in the present work contradicts other studies, concluding that other factors, such as the distance between the nozzle and the cross-linking bath significantly affect the sphericity factor. Some researchers have successfully produced high sphericity factor of alginate beads using a low concentration alginate solution by adjusting the distance (Lee *et al.,* 2013). According to the study, increasing the distance will give a longer relaxation time for the droplet to form better sphericity (Lee *et al.,* 2013).

During the detachment of the alginate solution from the nozzle tip, there is a gravitational force causing shape transition of the droplet in the tear, egg, and spherical shape, that can be easily differentiated when the distance between the nozzle and the cross-linking solution is longer (Lee *et al.,* 2013). When the alginate droplets impact the calcium chloride surface, deformation of the droplets occurs. After that, the alginate droplets detach from the surface of the calcium chloride solution-to-air surface due to surface tension and reform their spherical shape (Meiser *et al.,* 2009; Lee *et al.,* 2013). Other similar studies demonstrated that the deformation of the droplet during the collision of a droplet with the crosslinking solution could be affected by the nozzle and cross-linking solution (Chan *et al.,* 2009). However, the reshaping of the alginate droplet into a spherical shape is dependent on the viscosity of the alginate solution (Chan *et al.,* 2009; Shi *et al.,* 2011).

Optimisation of sphericity coefficient and model validation

The sphericity coefficient value closest to 1 signifies that the shape of the beads is more spherical. The highest value of the sphericity coefficient predicted was 0.763 under optimum conditions. Based on the results of the optimised sample and two samples chosen randomly as model validation, the calculated sphericity coefficients were 0.776, 0.791, and 0.809, respectively. The percentage difference between these samples was 1.68, 8.78, and 5.72%, respectively. It can be inferred that the relative percentage error between the predicted and experimental results in this experiment was less than 10%. Therefore, the correlation of the sphericity coefficient between the predicted and experimental results was reliable and well within the experimental error.

Simultaneous optimisation of particle size and sphericity coefficient of the alginate-pectin beads

Investigation of the optimal conditions for minimum alginate-pectin bead diameter and maximum sphericity coefficient were determined based on Design Expert® software. It was revealed that the optimal conditions involved four experimental variables: alginate-pectin concentration of 3.5%, flow rate of 10.00 mL/h, applied voltage of 2.4 kV, and distance between nozzle and cross-linking solution of 16 cm. Under this optimisation, alginate-pectin beads with an average diameter of 2.97 mm and sphericity coefficient of 0.776 were successfully achieved.

Conclusion

The primary goal of the present work was to illustrate the correlation between variables manipulated while electrospraying, and the diameter and sphericity coefficient of alginate-pectin beads.

The employment of CCD and RSM presented several advantages in enhancing the accuracy and providing the capability to link critical process parameters (CPPs) such as biopolymer concentration, applied voltage, flow rate, and distance between the nozzle and the cross-linking bath. The evidence from the present work suggested that the diameter of the alginate-pectin beads markedly influenced the applied voltage, while alginate-pectin solution concentration significantly impacted on the sphericity coefficient. On top of that, the present work reiterates the earlier hypothesis that the particle size and sphericity coefficient of alginate-pectin beads can be evoked by the interacting behaviour of some process variables. Among these, alginate-pectin concentration and flow rate have the highest importance in interaction in comparison to the other mutual effects in determining the diameter of the alginate-pectin beads. These findings enhance our understanding of the developed model used in predicting the size and shape behaviour of alginate-pectin beads for any given set of manipulated variables as well as recommend the optimised manipulated variables to attain ideal spherical beads of discrete size by the electrospray technique. To maximise the full potential of the alginate-pectin beads as biopolymer carriers, future research should endeavour to encapsulate food and medicinal particles *in vitro* and *in vivo*.

Acknowledgements

The present work was financially supported by the International Islamic University Malaysia (grant no.: IRAGS18-042-0043). The authors gratefully acknowledge the Laboratory of Advanced Drug Delivery, Kulliyyah of Pharmacy, International Islamic University Malaysia, Kuantan Campus, and Central Lab, Universiti Malaysia Pahang, Gambang Campus for the technical support received.

References

Abang, S., Chan, E. S. and Poncelet, D. 2012. Effects of process variables on the encapsulation of oil in ca-alginate capsules using an inverse gelation technique. Journal of Microencapsulation 29(5): 417-428.

Abyadeh, M., Zarchi, A. A. K., Faramarzi, M. A. and Amani, A. 2017. Evaluation of factors affecting size and size distribution of chitosan-electrosprayed nanoparticles. Avicenna Journal of Medical Biotechnology 9(3): 126-132.

Aguilar, K. C., Tello, F., Bierhalz, A. C., Romo, M. G. G., Flores, H. E. M. and Grosso, C. R. 2015. Protein adsorption onto alginate-pectin microparticles and films produced by ionic gelation. Journal of Food Engineering 154: 17-24.

Anuar, N., Mohd Adnan, A. F., Saat, N., Aziz, N. and Mat Taha, R. 2013. Optimization of extraction parameters by using response surface methodology, purification, and identification of anthocyanin pigments in *Melastoma malabathricum* fruit. The Scientific World Journal 2013: article ID 810547.

Bock, N., Dargaville, T. R. and Woodruff, M. A. 2012. Electrospraying of polymers with therapeutic molecules: state of the art. Progress in Polymer Science 37(11): 1510-1551.

Bock, N., Woodruff, M. A., Hutmacher, D. W. and Dargaville, T. R. 2011. Electrospraying, a reproducible method for production of polymeric microspheres for biomedical applications. Polymers 3(1): 131-149.

Chakraborty, S. 2017. Carrageenan for encapsulation and immobilization of flavor, fragrance, probiotics, and enzymes: a review. Journal of Carbohydrate Chemistry 36(1): 1-19.

Chan, E. S., Lee, B. B., Ravindra, P. and Poncelet, D. 2009. Prediction models for shape and size of ca-alginate macrobeads produced through extrusion-dripping method. Journal of Colloid and Interface Science 338(1): 63-72.

Coelho, T. L. S., Braga, F. M. S., Silva, N. M. C., Dantas, C., Júnior, C. A. L., de Sousa, S. A. A. and Vieira, E. C. 2019. Optimization of the protein extraction method of goat meat using factorial design and response surface methodology. Food Chemistry 281: 63-70.

Dekkers, B. L., Kolodziejczyk, E., Acquistapace, S., Engmann, J. and Wooster, T. J. 2016. Impact of gastric pH profiles on the proteolytic digestion of mixed βlg-Xanthan biopolymer gels. Food and Function 7(1): 58-68.

Ghelich, R., Jahannama, M. R., Abdizadeh, H., Torknik, F. S. and Vaezi, M. R. 2019. Central composite design (CCD)-Response surface methodology (RSM) of effective electrospinning parameters on PVP-B-Hf hybrid nanofibrous composites for synthesis of HfB_2-based composite nanofibers. Composites Part B: Engineering 166: 527-541.

Guo, J. and Kaletunç, G. 2016. Dissolution kinetics of pH responsive alginate-pectin hydrogel particles. Food Research International 88: 129-139.

Guo, J., Giusti, M. M. and Kaletunç, G. 2018. Encapsulation of purple corn and blueberry

extracts in alginate-pectin hydrogel particles: impact of processing and storage parameters on encapsulation efficiency. Food Research International 107: 414-422.

Houghton, M. E. and Amidon, G. E. 1992. Microscopic characterization of particle size and shape: an inexpensive and versatile method. Pharmaceutical Research 9(7): 856-859.

Jafari, M., Rahimi, M. R., Ghaedi, M., Javadian, H. and Asfaram, A. 2017. Fixed-bed column performances of azure-II and auramine-O adsorption by *Pinus eldarica* stalks activated carbon and its composite with zno nanoparticles: optimization by response surface methodology based on central composite design. Journal of Colloid and Interface Science 507: 172-189.

Kennedy, J. R., Kent, K. E. and Brown, J. R. 2015. Rheology of dispersions of xanthan gum, locust bean gum and mixed biopolymer gel with silicon dioxide nanoparticles. Materials Science and Engineering C 48: 347-353.

Kilinc, D., Dennis, C. L. and Lee, G. U. 2016. Bio-nano-magnetic materials for localized mechanochemical stimulation of cell growth and death. Advanced Materials 28(27): 5672-5680.

Lee, B. B., Ravindra, P. and Chan, E. S. 2013. Size and shape of calcium alginate beads produced by extrusion dripping. Chemical Engineering and Technology 36(10): 1627-1642.

Lim, F. and Sun, A. M. 1980. Microencapsulated islets as bioartificial endocrine pancreas. Science 210(4472): 908-910.

Lim, G. P., Lee, B. B., Ahmad, M. S., Singh, H. and Ravindra, P. 2016. Influence of process variables and formulation composition on sphericity and diameter of Ca-alginate-chitosan liquid core capsule prepared by extrusion dripping method. Particulate Science and Technology 34(6): 681-690.

Lotfipour, F., Mirzaeei, S. and Maghsoodi, M. 2012. Evaluation of the effect of $CaCl_2$ and alginate concentrations and hardening time on the characteristics of *Lactobacillus acidophilus* loaded alginate beads using response surface analysis. Advanced Pharmaceutical Bulletin 2(1): 71.

Ma, Y., Björnmalm, M., Wise, A. K., Cortez-Jugo, C., Revalor, E., Ju, Y. and Porter, C. J. 2018. Gel-mediated electrospray assembly of silica supraparticles for sustained drug delivery. ACS Applied Materials and Interfaces 10(37): 31019-31031.

Mehregan, A., Kadkhodaee, R., Ghorani, B., Razzaq, H. and Tucker, N. 2016. Controlling the morphology and material characteristics of electrospray generated calcium alginate micro-hydrogels. Journal of Microencapsulation 33(7): 605-612.

Meiser, I., Müller, S. C., Gepp, M. M., Zimmermann, H. and Ehrhart, F. 2009. Quantitative high-speed video analysis of biopolymer encapsulated cells while capsule formation. In Proceeding of the 4th European Conference of the International Federation for Medical and Biological Engineering, p. 2255-2258. Berlin: Springer.

Oladipo, A. A. and Gazi, M. 2015. Nickel removal from aqueous solutions by alginate-based composite beads: central composite design and artificial neural network modelling. Journal of Water Process Engineering 8: e81-e91.

Partovinia, A. and Vatankhah, E. 2019. Experimental investigation into size and sphericity of alginate micro-beads produced by electrospraying technique: operational condition optimization. Carbohydrate Polymers 209: 389-399.

Setyawidati, N. A. R., Puspita, M., Kaimuddin, A. H., Widowati, I., Deslandes, E., Bourgougnon, N. and Stiger-Pouvreau, V. 2018. Seasonal biomass and alginate stock assessment of three abundant genera of brown macroalgae using multispectral high-resolution satellite remote sensing: A case study at Ekas Bay (Lombok, Indonesia). Marine Pollution Bulletin 131: 40-48.

Shi, P., He, P., Teh, T. K., Morsi, Y. S. and Goh, J. C. 2011. Parametric analysis of shape changes of alginate beads. Powder Technology 210(1): 60-66.

Sodeifian, G., Ardestani, N. S., Sajadian, S. A. and Ghorbandoost, S. 2016a. Application of supercritical carbon dioxide to extract essential oil from *Cleome coluteoides* Boiss: experimental, response surface and grey wolf optimization methodology. The Journal of Supercritical Fluids 114: 55-63.

Sodeifian, G., Ghorbandoost, S., Sajadian, S. A. and Ardestani, N. S. 2016b. Extraction of oil from *Pistacia khinjuk* using supercritical carbon dioxide: experimental and modeling. The Journal of Supercritical Fluids 110: 265-274.

Thien, D. V. H., Hsiao, S. W. and Ho, M. H. 2012. Synthesis of electrosprayed chitosan nanoparticles for drug sustained release. Nano Life 2(1): article ID 1250003.

Valente, J. F. A., Dias, J. R., Sousa, A. and Alves, N. 2019. Composite central face design — an approach to achieve efficient alginate microcarriers. Polymers 11(12): article no. 1949.

Vicini, S., Castellano, M., Mauri, M. and Marsano, E. 2015. Gelling process for sodium alginate: new technical approach by using calcium rich micro-spheres. Carbohydrate Polymers 134: 767-774.

Voo, W. P., Ooi, C. W., Islam, A., Tey, B. T. and Chan, E. S. 2016. Calcium alginate hydrogel beads with high stiffness and extended dissolution behaviour. European Polymer Journal 75: 343-353.

Walkenström, P., Kidman, S., Hermansson, A. M., Rasmussen, P. B. and Hoegh, L. 2003. Microstructure and rheological behaviour of alginate/pectin mixed gels. Food Hydrocolloids 17(5): 593-603.

Yeo, J. C. and Lim, C. T. 2016. Emerging flexible and wearable physical sensing platforms for healthcare and biomedical applications. Microsystems and Nanoengineering 2: article no. 16043.